Biochemical and Biophysical Research Communications 432 (2013) 135–140

Contents lists available at SciVerse ScienceDirect

Biochemical and Biophysical Research Communications

journal homepage: www.elsevier.com/locate/ybbrc

Molecular cloning and characterization of a novel isoform of the non-canonical poly(A) polymerase PAPD7

Koichi Ogami, Rihe Cho, Shin-ichi Hoshino *

Department of Biological Chemistry, Graduate School of Pharmaceutical Sciences, Nagoya City University, Nagoya 467-8603, Japan

ARTICLE INFO

Article history:
Received 11 January 2013
Available online 29 January 2013

Keywords:
Polyadenylation
PAPD5
PAPD7
Non-canonical poly(A) polymerase
Nucleotidyl transferase
Trf4

ABSTRACT

Non-canonical poly(A) polymerases (ncPAPs) catalyze the addition of poly(A) tail to the 3′ end of RNA to play pivotal roles in the regulation of gene expression and also in quality control. Here we identified a novel isoform of the 7th member of ncPAPs: PAPD7 (PAPD7 l), which contains 230 extra amino acids at the amino terminus of the previously identified PAPD7 (PAPD7 s). In sharp contrast to the inactive PAPD7 s, PAPD7 l showed robust nucleotidyl transferase activity when tethered to an RNA. A region required for the activity was localized to 187–219 aa, and this region was also required for the nuclear retention of PAPD7 l. Western blot analysis revealed that 94 kDa band (corresponding to PAPD7 l) but not 62 kDa band (corresponding to PAPD7 s) detected by PAPD7 antibody was specifically depleted by treatment with PAPD7 siRNA in both HeLa and U2OS cells. These results suggest that PAPD7 l is the major and active isoform of PAPD7 expressed in cells.

1. Introduction

Mammalian cells contain genes for seven proteins of the non-canonical poly(A) polymerases (ncPAPs) or the Cid1-like family [1]. All these members as well as canonical poly(A) polymerases belong to the polymerase β-like nucleotidyl transferase superfamily. The family members have sequence and structural homology with the catalytic domain of DNA Pol β [2]. The general signature of this highly conserved catalytic-site motif is hG[GS]$x_{(7-13)}$-Dh[DE]h, with h indicating hydrophobic and x any amino acid. Two catalytic Asp and Glu residues in this motif are involved in the coordination of the divalent metal ion as a cosubstrate (such as $MgATP_{2-}$).

Trf4p and Trf5p, the only ncPAPs found in *S. cerevisiae*, are the component of TRAMP (Trf4/5p-Air1/2p-Mtr4p polyadenylation complex) and involved in nuclear RNA surveillance [3,4]. The TRAMP complex recognizes a variety of nuclear transcripts, such as snRNAs, snoRNAs, rRNAs, tRNAs, telomeric, and cryptic unstable transcripts (CUTs) [5–14]. Trf4/5p polyadenylates nuclear RNAs to facilitate their degradation by the nuclear exosome or their processing by the exosome-mediated 3′ end trimming [10,15,16].

PAPD5 and PAPD7 (also known as POLS or Trf4-1) were identified on the basis of sequence comparison with the yeast Trf4p [1,17]. PAPD5 was reported to function in the polyadenylation-mediated degradation of aberrant pre-rRNA [18], uridylation-dependent degradation of histone mRNAs [19] and the oligo(A) tail addition of snoRNA [20]. Like yeast Trf4p, PAPD5 forms a complex with MTR4, RRP6 and a human ortholog of yeast Air1p, ZCCHC7 [21,22], suggesting the existence of a TRAMP-like complex in humans. Whereas Trf4p is inactive by itself and requires Air1/2p to polyadenylate RNA substrates [3,7], PAPD5 was shown to be able to bind to RNA substrates directly and catalyze the polyadeylation in the absence of a protein cofactor [23]. In contrast to PAPD5, neither enzymatic characteristics nor biological functions of PAPD7 have been described.

In this study, we generated PAPD7-specific antibodies and found that PAPD7 protein migrated at about 94 kDa on SDS–PAGE, which was slower than the NCBI's Entrez protein (NP_001165276) migrated at about 62 kDa. The 94 kDa isoform of PAPD7 has N-terminal extension, which is encoded by highly GC-rich sequence (>76%). Fluorescent microscopy analysis revealed that PAPD5 and 94 kDa PAPD7 display different intranuclear distributions: PAPD5 accumulates in the nucleoli, whereas PAPD7 is excluded from the nucleoli. A minor pool of PAPD7 was observed in the cytoplasm. We also confirmed the nucleotidyl transferase activities of these proteins by tethering assays. Intriguingly, the 94 kDa PAPD7 exhibits a robust nucleotidyl transferase activity compared with the 62 kDa isoform when tethered to mRNA 3′UTR, although both of which contain nucleotidyl transferase domain. The nucleotidyl transferase activity of 94 kDa PAPD7 was comparable to that of PAPD5. Comparison between PAPD5 and PAPD7 N-terminal sequences revealed that these regions contain conserved residues

Abbreviations: ncPAP, noncanonical poly(A) polymerase; NES, nuclear export signal; NLS, nuclear localization signal; NTD, nucleotidyl transferase domain; CUT, cryptic unstable transcripts; siRNA, small interfering RNA; LMB, leptomycin B.

* Corresponding author. Fax: +81 52 836 3427.
E-mail address: hoshino@phar.nagoya-cu.ac.jp (S.-i. Hoshino).

0006-291X/$ - see front matter © 2013 Elsevier Inc. All rights reserved.
http://dx.doi.org/10.1016/j.bbrc.2013.01.072

that were juxtaposed to nucleotidyl transferase domain. Finally, we narrowed the N-terminal region that is indispensable for the nucleotidyl transferase activity and nuclear localization of PAPD7. Our results point out the possibilities that PAPD7 as well as PAPD5 has strong nucleotidyl transferase activity that is conferred by the N-terminal region and that these proteins polyadenylate different RNAs.

2. Materials and methods

2.1. Plasmid construction

The coding sequences of PAPD5 (NM_001040284) and PAPD7 (NM_006999.4) were amplified from U2OS cDNA library, and cloned into pCMV-Myc (Clontech) or pCMV-5×Myc [24]. For the cloning of N-terminally extended PAPD7, primers 5′ TTG GAA TTC ATG CAG ATC TGG GAG ACC 3′ was used to amplify from −690 ATG. To construct pCI-neo-λN, inverse PCR was performed to introduce the Kozak sequence followed by N22 peptide coding sequence between the *NheI* and *EcoRI* sites of pCI-neo (Clontech). The coding sequences of 5×Myc-PAPD5, 5×Myc-PAPD7 or 5×Myc were PCR-amplified and inserted into pCI-neo-λN. Point mutants or deletion mutants were generated by inverse PCR. Note that as the nucleotide sequence between −690 ATG to +1 ATG of PAPD7 l is highly GC-rich, PCR reactions were performed using KOD plus ver.2 (Takara) in the presence of 5% DMSO or KOD FX (Takara). PCR reactions for sequencing analyses were also performed in the presence of 5% DMSO. pFlag-CMV5/TO-BGG boxB was generated by inserting 30nt spacer sequence followed by boxB sequence after BGG stop codon. To construct pBSII-5×Flag-7SK, 7SK gene including the proximal sequence element (PSE) and the TATA box was cloned into pBSII. Fag-tag sequence was inserted into 5′ end of the 7SK-coding sequence.

2.2. Antibodies

Antibodies used in this study were the following: anti-c-Myc (9E10, Roche), anti-GAPDH (6C5, Millipore), anti-C23 (H-250, Santa Cruz). Anti-PAPD5 and anti-PAPD7 were raised against His-tagged PAPD5 (517–698 a.a; NP_001035374) and PAPD7 (308–542 a.a; NP_001165276), respectively.

2.3. siRNA

The sequence of siRNA for luciferase was previously described [24]. PAPD5 and PAPD7 siRNA consisted of 5′ r (GGACGACACUU-CAAUUAUU) d(TT) 3′and 5′ r (GAAUUACAUGAAGAAAUAU) d(TT) 3′, respectively.

2.4. Cell culture and transfection

HeLa and U2OS cells were cultured in Dulbecco's modified Eagle's medium (Nissui) supplemented with 5% fetal bovine serum. Transfection of plasmid DNA was performed using Lipofectamine 2000 (Invitrogen) as described previously [25]. For siRNA transfection, Lipofectamine RNAi MAX (Invitrogen) was used.

2.5. Northern analysis

The northern blotting analysis was performed as described previously [24].

2.6. Immunolocalization analysis

Localization of PAPD5, PAPD7 and PAPD7 mutants were visualized in HeLa cells. Twenty-four hours after transfection, cells were washed once with PBS, fixed with 4% paraformaldehyde in PBS for 12 min, quenched with 10 mM Glycine in PBS for 10 min, permiabilized with 0.1% Triton X-100, 1% goat serum in PBS for 12 min, and incubated at 4 °C overnight with primary mouse anti-Myc (1:400) and rabbit anti-C23 (1:100) antibodies. Cells were then washed three times with PBS for 10 min and incubated with Alexa Fluor 488 goat anti-mouse antibody (1:200), Alexa Fluor 568 anti-rabbit antibody (1:200) and DAPI. Images were obtained using an OLYMPUS IX71 fluorescent microscope.

2.7. Accession number

The nucleotide and deduced amino acid sequence of PAPD7 l are available at GenBank (accession number KC424495).

3. Results

3.1. Identification of N-terminaly extended PAPD7 isoform

It has already been shown that PAPD5 catalyzes polyadenylation of RNA substrates *in vitro* [23]. As PAPD7 deposited in NCBI protein database shares strong identity with PAPD5 (>77%) especially in the nucleotidyl transferase domain (>92%) and PAP-associated domain (>94%), we first examined the nucleotidyl transferase activity of PAPD7 as well as PAPD5 by using MS2-based tethering strategy. HeLa cells were co-transfected with β-globin (BGG) MS2-bs reporter gene and a plasmid expressing MS2-fused PAPD5 or PAPD7. Unexpectedly, we could not detect any significant activity for PAPD7, which is in sharp contrast to PAPD5 (data not shown). Therefore, PAPD7-specific antibodies were generated in two individual rabbits using recombinant PAPD7 (C-terminal 235 a.a. of NP_001165276) prepared from *E.coli* as antigen (Fig. 1A). Western blot analysis of HeLa or U2OS cell extracts revealed that proteins commonly detected by these antibodies migrated at about 94 kDa, which was slower than the NCBI's Entrez protein (NP_001165276) migrated at about 62 kDa on SDS–PAGE (Fig. 1B and data not shown). Since 94 kDa protein was specifically depleted by treatment with siRNA against PAPD7, the NP_001165276 clone is unlikely to contain full-length PAPD7. Computational analysis of the 5′-flanking region of PAPD7 gene coding for the NCBI's Entrez mRNA (NM_006999) revealed that it has a candidate AUG triplet corresponding to the size of the 94 kDa form of PAPD7 (Supplementary Figure, positions −690 of the proposed AUG (+1)). To determine whether the upstream AUG is actually transcribed and used as the translation initiation site to produce full-length PAPD7, a primer was designed to amplify cDNA starting from the putative initiation site. The primer −690 ATG successfully amplified PAPD7 cDNA with extended 5′ sequence from a U2OS cDNA library. It is note that this PCR product was not amplified from contaminated genomic DNA as an isolated amplicon contains exon-exon junctions. To test if PAPD7 cDNA with the extended 5′ sequence indeed encodes 94 kDa form of PAPD7, this amplicon was cloned into pCMV-Myc and expressed exogenously in HeLa cells. Western blot analysis using anti-PAPD7 antibody showed that the exogenously expressed protein migrated at a similar position to endogenous PAPD7 (Fig. 1C). From these results, we conclude that the 94 kDa form of PAPD7 (hereafter referred to as PAPD7 l) has N-terminal extension compared to the NCBI's Entrez protein NP_001165276 (hereafter referred to as PAPD7 s).

Thus, we next examined nucleotidyl transferase activity of the newly identified PAPD7 l by using λN-boxB-based tethering system. The assay was performed by co-transfecting with β-globin

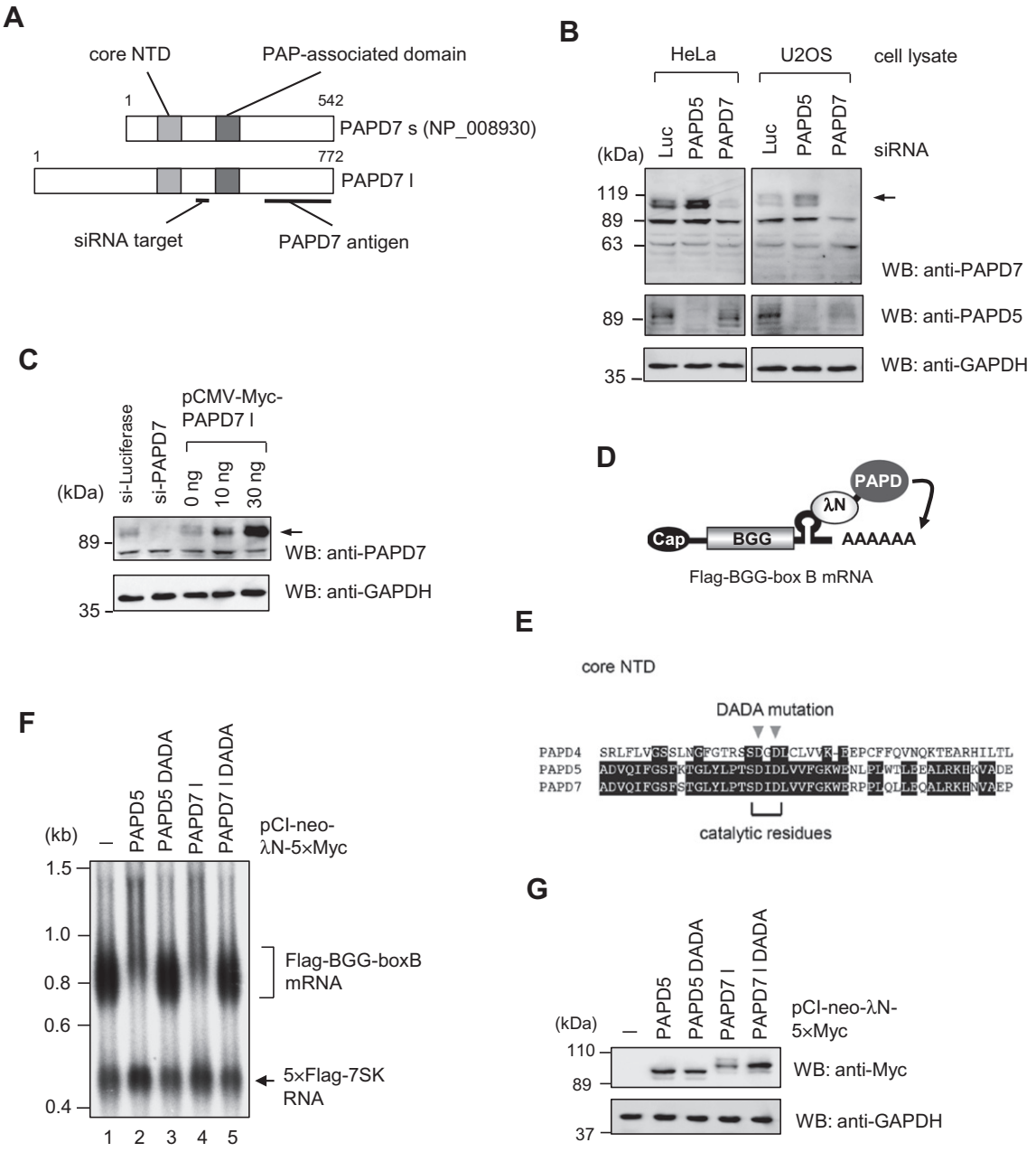

Fig. 1. Identification of 94 kDa PAPD7 isoform. (A) Scheme of original PAPD7 clone (NP_008930.1). The light- and dark-gray boxes indicate core NTD and PAP-associated domain, respectively. The areas used for antibody production and siRNA knockdown are underlined. (B) HeLa or U2OS cells were transfected with PAPD5, PAPD7 or control Luciferase siRNA for 72 h. Cell lysates were analyzed by western blotting using the indicated antibodies. An arrow indicates the protein specifically depleted by si-PAPD7.(C) HeLa cells were transfected with siRNA against PAPD7 or control Luciferase, or increasing amount of pCMV-Myc-PAPD7. Exogeous PAPD7 protein migrated at almost the same position to endogenous PAPD7 on SDS–PAGE. (D) Tethered function assays using λN-boxB-based tethering system. λN-fused PAPD proteins were brought to 3′UTR of a BGG boxB reporter mRNA, and the nucleotidyl transferase activity was examined. (E) Sequence alignment of the core nucleotidyl transferase domain of PAPD4, PAPD5 and PAPD7. Identical residues are *shaded* in *black*. (F) HeLa cells were transfected with pFlag-CMV5/TO-BGG boxB reporter plasmid, pBSII-5×Flag-7SK reference plasmid, and either pCI-neo-λN-5×Myc-PAPD5, pCI-neo-λN-5×Myc-PAPD7, or their DADA mutants. Total RNAs were prepared from the cells and subjected to northern blotting. (G) Total cell lysates were analyzed by western blotting using the indicated antibodies.

(BGG) boxB reporter and a plasmid encoding either λN-fused test protein or its mutated form (DADA) (Fig. 1D and E). Multiple Flag-tagged 7SK RNA served as transfection/loading control. When PAPD7 l was tethered to the mRNA 3′UTR, the protein displayed strong nucleotidyl transferase activity, which was comparable to that of PAPD5 (Fig. 1F, lanes 2 and 4). Mutations of two aspertate residues in the nucleotidyl transferase domain (DADA) completely abolished the nucleotidyl transferase activity of these proteins (lanes 3 and 5). The expression level of tethered proteins was confirmed by western blotting (Fig. 1G). The same result was obtained when MS2-based tethering system was used instead of λN-boxB system (data not shown).

3.2. Differential subcellular localization of PAPD5 and PAPD7

We next examined the subcellular localization of PAPD5 and PAPD7. N-terminally Myc-tagged proteins were visualized in transiently transfected HeLa cells. To discriminate between the nucleolar and nonnucleolar part, we stained nucleolar part with anti-nucleolin antibody (NCL). As previously described [21,23],

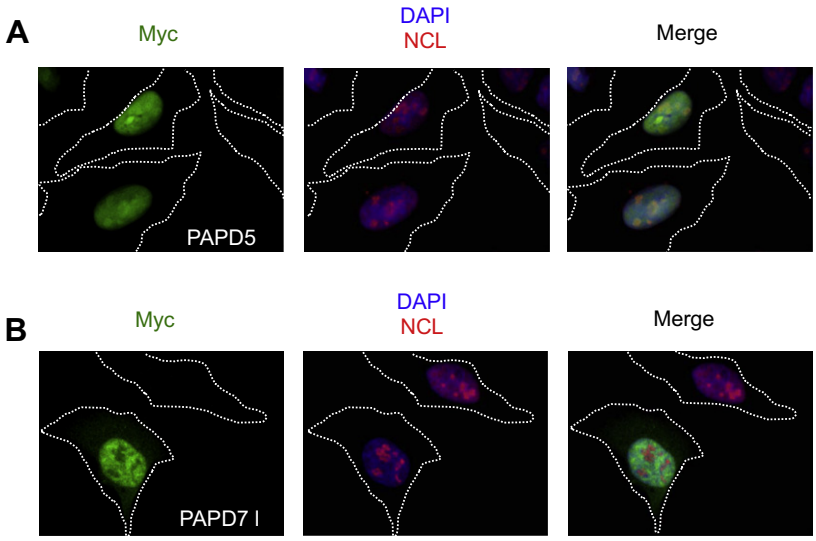

Fig. 2. Different subcellular localization of PAPD5 and PAPD7. HeLa cells were transfected with pCMV-Myc-PAPD5 (A) or pCMV-Myc-PAPD7 l (B), and the localization of expressed proteins were analyzed by immunofluorescence using anti-Myc antibody and visualized by fluorescent microscopy (green). Nucleolin (NCL) staining (red) served as a nucleolar marker and was overlaid with labeling of nuclei by DAPI (blue).

PAPD5 localized strictly to the nucleus with nucleolar accumulation as judged by the co-localization with nucleolin (Fig. 2A). PAPD7 mainly localized to the nucleus, however, in sharp contrast to PAPD5, it was excluded from the nucleolus and weak staining was detected in the cytoplasm (Fig. 2B). Similar results were obtained for U2OS cells (data not shown). These results suggest that in contrast to PAPD5, which functions in the nucleus, PAPD7 functions mainly in the nucloplasm, and also has roles in the cytoplasm.

3.3. Newly identified N-terminal region is indispensable for both the nucleotidyl transferase activity and the nuclear localization of PAPD7

As described above, we have observed that tethering of PAPD7 l but not PAPD7 s that lacks N-terminal region (NP_001165276) results in extensive nucleotide transfer to mRNA substrates (Fig. 3B, PAPD7 l and s). These facts imply that there is a region that is indispensable for catalytic activity of PAPD7 in the newly identified N-terminal region, besides the nucleotidyl transferase domain and PAP-associated domain. To search for such a region, we first compared the N-terminal sequence of PAPD7 l with its corresponding region of PAPD5 and identified a highly conserved sequence that is located in juxtaposition to nucleotidyl transferase domain (Fig. 3A). The sequence identified is absent in other non-canonical poly(A) polymerases. Deletion of this region completely abolished the nucleotidyl transferase activity of PAPD7 (Fig. 3B, Δ1). To further narrow the area, we prepared a set of deletion constructs (Fig. 3A, Δ2–Δ4). PAPD7 residues 167–186 which contain a stretch of basic amino acids are dispensable for the nucleotidyl transferase activity (Fig. 3A and B, Δ2). In contrast, PAPD7 lacking residues 187–230 did not show nucleotidyl transferase activity (Δ3). The Δ4 mutant that lacks residues 187–219 but contains residues 220–230 which are conserved in PAPD5 and yeast Trf4 protein was not able to transfer nucleotides to the reporter mRNA. The expression level of tethered proteins was confirmed by western blotting (Fig. 3C). Taken together, we conclude that not only core NTD but also residues 187–219 are required for the full nucleotidyl transferase activity of PAPD7.

In addition to the difference in the nucleotidyl transferase activity between PAPD7 l and PAPD7 s, we found that these proteins exhibit different distribution in cells (Fig. 3D and E). PAPD7 l was more abundant in the nucleus than the cytoplasm, whereas PAPD7 s that lacks N-terminal residues evenly distributed throughout the cell. To investigate the region responsible for the nuclear localization of PAPD7 l, we utilized the deletion mutants (Δ1–Δ4). Unexpectedly, the same distribution as PAPD7 l was observed only in Δ2 mutant, although the mutant lacks a putative nuclear localization signal (NLS)-like sequence (RRKR). In contrast, other mutants showed strong cytoplasmic localization (Δ1, Δ3 and Δ4), indicating that PAPD7 residues 187–219 are required for the nuclear localization of PAPD7.

4. Discussion

In this report, we have identified a novel N-terminally extended 94 kDa isoform of PAPD7 (PAPD7 l). Translation of this isoform starts at AUG codon located at 690 nt upstream from the previously predicted start codon of NCBI's Entrez mRNA (NM_006999) which encodes 62 kDa isoform of PAPD7 (PAPD7 s). Interestingly, the PAPD7 l but not PAPD7 s exhibits nucleotidyl transferase activity. This finding and the fact that only 94 kDa protein was specifically depleted by siRNA against PAPD7 in both HeLa and U2OS cells indicate that the PAPD7 l is the major and active isoform that is actually expressed in cells.

The observation that PAPD7 l but not PAPD7 s showed catalytic activity was surprising, because both isoforms contain nucleotidyl transferase domain. Analysis of deletion mutants revealed the importance of residues 187–219 for the nucleotidyl transferase activity of PAPD7 l. This region is also required for nuclear localization of PAPD7 l. It appears that nuclear retention of PAPD7 l correlates with the nucleotidyl transferase activity; the deletion mutants that lost its catalytic activity have a tendency to localize in the cytoplasm. Since no putative NLS was found in this region, we hypothesize that this region is involved in the interaction with other factors that is required for nuclear retention and the nucleotidyl transferase activity of PAPD7 l.

While PAPD7 l lacking residues 167–230 (Δ1) is almost exclusively cytoplasmic, PAPD7 l lacking residues 1–230 (PAPD7 s) is evenly distributed throughout the cell. These results led us to speculate that PAPD7 l contains a nuclear export signal (NES) in residues 1–166. We therefore treated cells with a nuclear export inhibitor, leptomycin B (LMB) and examined subcellular

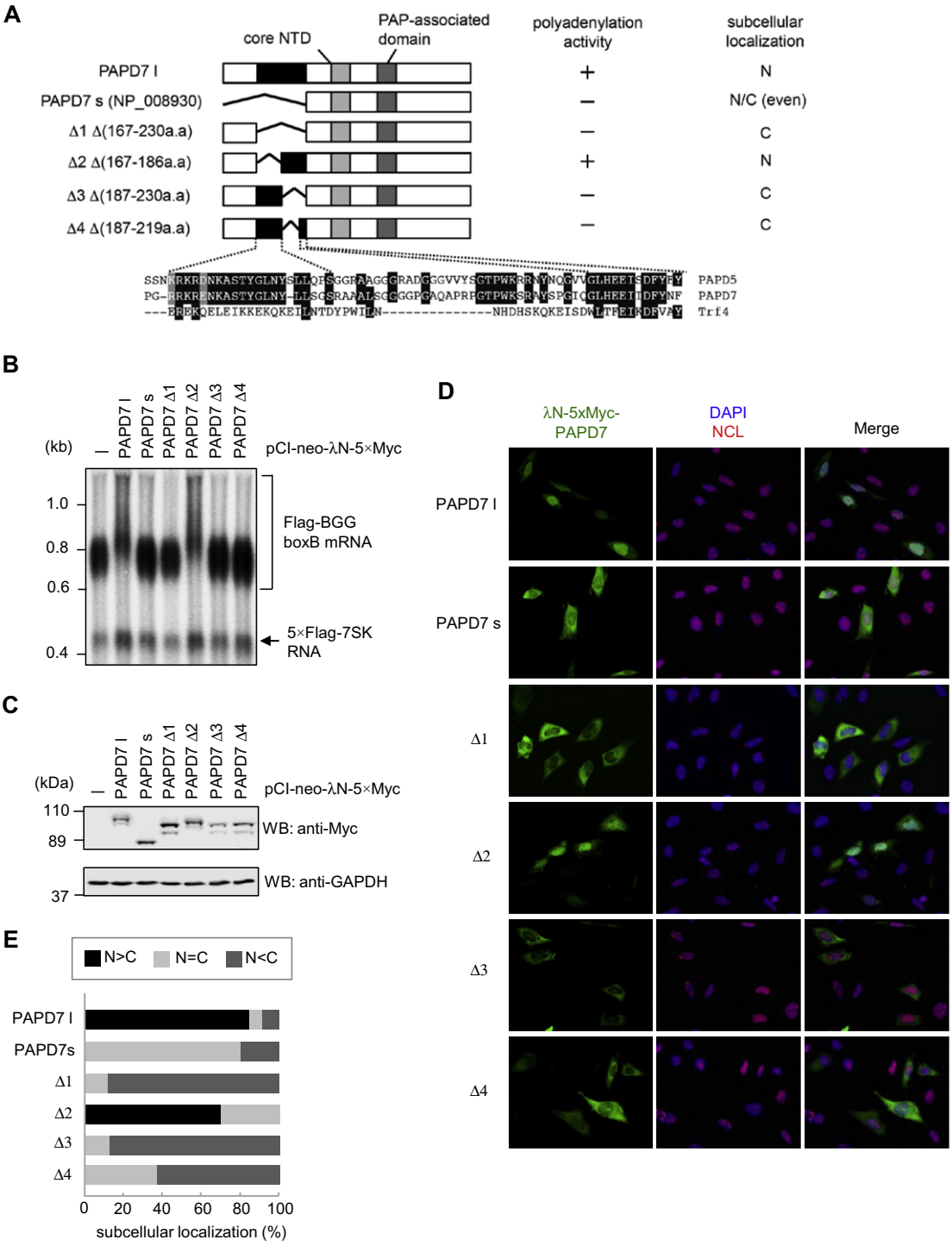

Fig. 3. Identification of an N-terminal region that is indispensable for both the nucleotidyl transferase activity and nuclear localization. (A) Overview of mutant forms of PAPD7 proteins used in this study. The core nucleotidyl transferase domain (core NTD) and PAP-associated domain are indicated by the light and dark gray boxes, respectively. The black box indicates the region that is conserved between PAPD5 and PAPD7, and its sequence alignments were shown below. The summary of the nucleotidyl transferase activity and the subcellular localization of these proteins are shown on the right. (B) HeLa cells were transfected with pFlag-CMV5/TO-BGG boxB reporter plasmid, pBSII-5×Flag-7SK reference plasmid, and either pCI-neo-λN-5×Myc-PAPD7 or its deletion mutants. Total RNAs were prepared from the cells and subjected to northern blotting. (C) Total cell lysates were analyzed by western blotting using indicated antibodies. (D) HeLa cells were transfected with pCI-neo-λN-5×Myc-PAPD7 or its deletion mutants and the localization of expressed proteins were analyzed by immunofluorescence using anti-Myc antibody and visualized by fluorescent microscopy (green). Nucleolin (NCL) staining (red) served as a nucleolar marker and was overlaid with labeling of nuclei by DAPI (blue). (E) Histogram showing the intracellular distribution of each construct. Shown is the proportion in each compartment, using measurements from 48–71 cells for each construct.

localization of Δ1 mutant. However, LMB treatment did not cause nuclear accumulation of the mutant: Δ1 mutant remain cytoplasmic after the incubation with LMB (data not shown). Thus, it is unlikely that the cytoplasmic localization of PAPD7 mutants is the result of Crm1-dependent nuclear export.

An interesting and important observation is that PAPD7 and its paralog PAPD5 display different intracellular distributions. PAPD5, in agreement with previously published results, is restricted to the nucleus with nucleolar enrichment [21]. In contrast, the majority of PAPD7 is nuclear but excluded from nucleoli. We also confirmed

a minor cytoplasmic pool of PAPD7. We therefore propose that the biological functions of these paralogs are not equivalent. In support of this proposal, previous study demonstrated that PAPD5 but not PAPD7 is responsible for the polyadenylation of aberrant pre-rRNAs in mouse cells [18] and in human cells (our unpublished data). We note that despite the previous work using PAPD7 s [22], we were unable to confirm the interaction between PAPD7 and ZCCHC7 (data not shown). As ZCCHC7 was shown to display a strict nucleolar localization [21,22], and as PAPD7 s is also excluded from nucleoli, we think it is unlikely that PAPD7 forms complex with ZCCHC7. On the other hand, we could detect the interaction between PAPD5 and ZCCHC7 (as described previously [21] and data not shown) indicating that PAPD5 is truly a component of the nucleolar TRAMP-like complex in human cells.

The functional relevance of PAPD7 as well as PAPD5 outside nucleoli remains to be elucidated, however, several evidences point out the possibility that PAPD7 and/or PAPD5 are also involved in the pre-mRNA processing in the nucleoplasm. First, PAPD7 s was shown to interact with a non-nucleolar protein PRPF31 that is necessary for U4/U6•U5 tri-snRNP formation [26,27]. PAPD5 also interacts with a subset of splicing factors including PRPF31 [21]. Second, in budding yeast, the function of Trf4p is not restricted to ncRNA surveillance. It has been reported that Trf4p but not Trf5p is indispensable for the proper 3′ end formation of mRNAs encoding Nab2 [28] or Cth2 [29]. Future research will aim to identify the substantial substrate of PAPD7 and to determine whether PAPD7 and PAPD5 work redundantly or independently in the nucleoplasm.

Acknowledgments

This work was supported by a Grant-in-Aid for Scientific Research on Innovative Areas "RNA regulation" (No. 20112005) from the Ministry of Education, Culture, Sports, Science and Technology of Japan, and a Grant-in-Aid for Scientific Research (B) (No. 21370080) from Japan Society for the Promotion of Science (to S H).

Appendix A. Supplementary data

Supplementary data associated with this article can be found, in the online version, at http://dx.doi.org/10.1016/j.bbrc.2013.01.072.

References

[1] M.J. Schmidt, C.J. Norbury, Polyadenylation and beyond: emerging roles for noncanonical poly(A) polymerases, Wiley Interdiscip. Rev. RNA 1 (2010) 142–151.
[2] G. Martin, W. Keller, RNA-specific ribonucleotidyl transferases, RNA 13 (2007) 1834–1849.
[3] J. LaCava, J. Houseley, C. Saveanu, E. Petfalski, E. Thompson, A. Jacquier, D. Tollervey, RNA degradation by the exosome is promoted by a nuclear polyadenylation complex, Cell 121 (2005) 713–724.
[4] J. Houseley, D. Tollervey, Yeast Trf5p is a nuclear poly(A) polymerase, EMBO Rep. 7 (2006) 205–211.
[5] J.T. Arigo, D.E. Eyler, K.L. Carroll, J.L. Corden, Termination of cryptic unstable transcripts is directed by yeast RNA-binding proteins Nrd1 and Nab3, Mol. Cell 23 (2006) 841–851.
[6] M. Thiebaut, E. Kisseleva-Romanova, M. Rougemaille, J. Boulay, D. Libri, Transcription termination and nuclear degradation of cryptic unstable transcripts: a role for the nrd1-nab3 pathway in genome surveillance, Mol. Cell 23 (2006) 853–864.
[7] F. Wyers, M. Rougemaille, G. Badis, J.C. Rousselle, M.E. Dufour, J. Boulay, B. Regnault, F. Devaux, A. Namane, B. Seraphin, D. Libri, A. Jacquier, Cryptic pol II transcripts are degraded by a nuclear quality control pathway involving a new poly(A) polymerase, Cell 121 (2005) 725–737.
[8] C.A. Davis, M. Ares Jr., Accumulation of unstable promoter-associated transcripts upon loss of the nuclear exosome subunit Rrp6p in Saccharomyces cerevisiae, Proc. Natl. Acad. Sci. USA 103 (2006) 3262–3267.
[9] C. Dez, J. Houseley, D. Tollervey, Surveillance of nuclear-restricted pre-ribosomes within a subnucleolar region of Saccharomyces cerevisiae, EMBO J. 25 (2006) 1534–1546.
[10] D.E. Egecioglu, A.K. Henras, G.F. Chanfreau, Contributions of Trf4p- and Trf5p-dependent polyadenylation to the processing and degradative functions of the yeast nuclear exosome, RNA 12 (2006) 26–32.
[11] T. Carneiro, C. Carvalho, J. Braga, J. Rino, L. Milligan, D. Tollervey, M. Carmo-Fonseca, Depletion of the yeast nuclear exosome subunit Rrp6 results in accumulation of polyadenylated RNAs in a discrete domain within the nucleolus, Mol. Cell Biol. 27 (2007) 4157–4165.
[12] J. Houseley, K. Kotovic, A. El Hage, D. Tollervey, Trf4 targets ncRNAs from telomeric and rDNA spacer regions and functions in rDNA copy number control, EMBO J. 26 (2007) 4996–5006.
[13] S. San Paolo, S. Vanacova, L. Schenk, T. Scherrer, D. Blank, W. Keller, A.P. Gerber, Distinct roles of non-canonical poly(A) polymerases in RNA metabolism, PLoS Genet. 5 (2009) e1000555.
[14] K.P. Callahan, J.S. Butler, TRAMP complex enhances RNA degradation by the nuclear exosome component Rrp6, J. Biol. Chem. 285 (2010) 3540–3547.
[15] S. Kadaba, A. Krueger, T. Trice, A.M. Krecic, A.G. Hinnebusch, J. Anderson, Nuclear surveillance and degradation of hypomodified initiator tRNAMet in *S. cerevisiae*, Genes Dev. 18 (2004) 1227–1240.
[16] S. Vanacova, J. Wolf, G. Martin, D. Blank, S. Dettwiler, A. Friedlein, H. Langen, G. Keith, W. Keller, A new yeast poly(A) polymerase complex involved in RNA quality control, PLoS Biol. 3 (2005) e189.
[17] C. Walowsky, D.J. Fitzhugh, I.B. Castano, J.Y. Ju, N.A. Levin, M.F. Christman, The topoisomerase-related function gene TRF4 affects cellular sensitivity to the, J. Biol. Chem. 274 (1999) 7302–7308.
[18] N. Shcherbik, M. Wang, Y.R. Lapik, L. Srivastava, D.G. Pestov, Polyadenylation and degradation of incomplete RNA polymerase I transcripts in mammalian cells, EMBO Rep. 11 (2010) 106–111.
[19] T.E. Mullen, W.F. Marzluff, Degradation of histone mRNA requires oligouridylation followed by decapping and simultaneous degradation of the mRNA both 5′–3′ and 3′–5′, Genes Dev. 22 (2008) 50–65.
[20] H. Berndt, C. Harnisch, C. Rammelt, N. Stohr, A. Zirkel, J.C. Dohm, H. Himmelbauer, J.P. Tavanez, S. Huttelmaier, E. Wahle, Maturation of mammalian H/ACA box snoRNAs: PAPD5-dependent adenylation and PARN-dependent trimming, RNA 18 (2012) 958–972.
[21] M. Lubas, M.S. Christensen, M.S. Kristiansen, M. Domanski, L.G. Falkenby, S. Lykke-Andersen, J.S. Andersen, A. Dziembowski, T.H. Jensen, Interaction profiling identifies the human nuclear exosome targeting complex, Mol. Cell 43 (2011) 624–637.
[22] M.B. Fasken, S.W. Leung, A. Banerjee, M.O. Kodani, R. Chavez, E.A. Bowman, M.K. Purohit, M.E. Rubinson, E.H. Rubinson, A.H. Corbett, Air1 zinc knuckles 4 and 5 and a conserved IWRXY motif are critical for the function and integrity of the Trf4/5-Air1/2-Mtr4 polyadenylation (TRAMP) RNA quality control complex, J. Biol. Chem. 286 (2011) 37429–37445.
[23] C. Rammelt, B. Bilen, M. Zavolan, W. Keller, PAPD5, a noncanonical poly(A) polymerase with an unusual RNA-binding motif, RNA 17 (2011) 1737–1746.
[24] N. Hosoda, Y. Funakoshi, M. Hirasawa, R. Yamagishi, Y. Asano, R. Miyagawa, K. Ogami, M. Tsujimoto, S. Hoshino, Anti-proliferative protein Tob negatively regulates CPEB3 target by recruiting Caf1 deadenylase, EMBO J. 30 (2011) 1311–1323.
[25] Y. Funakoshi, Y. Doi, N. Hosoda, N. Uchida, M. Osawa, I. Shimada, M. Tsujimoto, T. Suzuki, T. Katada, S. Hoshino, Mechanism of mRNA deadenylation: evidence for a molecular interplay between translation termination factor eRF3 and mRNA deadenylases, Genes Dev. 21 (2007) 3135–3148.
[26] A. Nag, J.A. Steitz, Tri-snRNP-associated proteins interact with subunits of the TRAMP and nuclear, RNA Biol. 9 (2012) 334–342.
[27] O.V. Makarova, E.M. Makarov, S. Liu, H.P. Vornlocher, R. Luhrmann, Protein 61K, encoded by a gene (PRPF31) linked to autosomal dominant retinitis, EMBO J. 21 (2002) 1148–1157.
[28] K.M. Roth, J. Byam, F. Fang, J.S. Butler, Regulation of NAB2 mRNA 3'-end formation requires the core exosome and the Trf4p component of the TRAMP complex, RNA 15 (2009) 1045–1058.
[29] D. Ciais, M.T. Bohnsack, D. Tollervey, The mRNA encoding the yeast ARE-binding protein Cth2 is generated by a novel 3′ processing pathway, Nucleic Acids Res. 36 (2008) 3075–3084.